Surprising consequences of ion conservation in electro-osmosis over a surface charge discontinuity

ADITYA S. KHAIR AND TODD M. SQUIRES

Department of Chemical Engineering, University of California, Santa Barbara, CA 93106-5080, USA

A variety of microfluidic technologies utilise electrokinetic transport over rigid surfaces possessing rapid variations in charge. Here, as a paradigmatic model system for such situations, we consider electro-osmosis past a flat plate possessing a discontinuous jump in surface charge. Although the problem is relatively simple to pose, our analysis highlights a number of interesting and somewhat surprising features. Notably, the standard assumption that the electric field outside the diffuse screening layer is equal to the uniform applied field leads to a violation of ion conservation, since the applied field drives an ionic surface current along the diffuse layer downstream of the jump, whereas there is zero surface current upstream. Instead, at the surface charge discontinuity, field lines are drawn into the diffuse layer to supply ions from the bulk electrolyte, thereby ensuring ion conservation. A simple charge conservation argument reveals that the length-scale over which this process occurs is of the order of the ratio of surface-to-bulk electrolyte conductivities, $L_H = \sigma_s/\sigma_b$. For a highly charged surface, L_H can be several orders of magnitude greater than the Debye screening length λ_D, which is typically nanometres in size. Remarkably, therefore, nano-scale surface conduction may cause micrometre-scale gradients in the bulk electric field. After a distance $O(L_H)$ downstream, the bulk field 'heals' and is once again equal to the applied field. Scaling all distances with the 'healing length' L_H yields a universal set of equations for the bulk field and fluid flow, which are solved numerically. Finally, we discuss the role of surface conduction in driving a non-uniform ion distribution, or concentration polarization, in the bulk electrolyte.

1. Introduction

Electrokinetic effects involve the interaction of electric fields and hydrodynamic flows with the charged ionic screening clouds that surround solid surfaces in electrolytes (Russel, Saville & Schowalter 1989; Lyklema 1995). Although electrokinetics is a well-established field, dating back nearly two centuries to the pioneering electrophoresis experiments of Reuss (1809), the emergence of microfluidic technologies over recent decades has spurred a resurgence of interest (Stone, Stroock & Ajdari 2004; Squires & Quake 2005). For example, electro-osmotic flow provides an alternative to mechanical pressure-driven pumping of fluids through micrometre-scale channels (or smaller), with the advantage that flow rate does not scale down with channel size. Furthermore, electrokinetic transport plays a crucial role in lab-on-a-chip separations (Khandurina & Guttman 2003), charge-selective nanochannels (Wang, Stevens & Han 2005; Kim et al. 2007), and micro-scale energy conversion (van der Heyden et al. 2006; van der Heyden et al. 2007; Pennathur, Eijkel & van der Berg 2007). Additionally,

the ability to control geometry and surface properties in microfluidic devices has allowed for a new means of testing and improving on existing electrokinetic theories (e.g. Storey *et al.* 2008.)

In particular, the last few decades have witnessed increased attention to electrokinetics over inhomogeneously charged surfaces. Initial work by Teubner (1982) and Anderson (1985) focused on the electrophoretic motion of a freely suspended particle with non-uniform surface charge. More recently, Long & Ajdari (1998) investigated electrophoresis of particles with coupled charge and shape variations. Anderson & Idol (1985) considered electro-osmosis in a cylindrical pore with periodic axial variations in zeta potential, and found that the fluid flow contained eddies and re-circulation regions, in contrast to the unidirectional flow observed for a uniformly charged pore (Rice & Whitehead 1965). Stroock *et al.* (2000) measured electro-osmotic flow in a channel whose bottom wall was lithographically patterned with an alternating surface charge, thereby verifying the theoretical predictions of Ajdari (1995). Surface charge inhomogeneities also occur in micro-fabricated channels and capillaries owing to, for instance, contamination of the walls by adsorption of molecules in the surrounding fluid. On this theme, Long, Stone & Ajdari (1999) computed the electro-osmotic flow in planar and cylindrical capillaries created by defects in surface-charge distribution. The impact of non-uniform surface charge on dispersion in capillary electrophoresis has been reviewed by Ghosal (2006).

Discontinuous variations in surface charge are ubiquitous for an entire class of nonlinear electrokinetic systems involving patterned thin metal films, generally classified as induced-charge electrokinetics (ICEK). For example, Ramos *et al.* (1998) and González *et al.* (2000) showed that an a.c. field applied across two narrowly spaced co-planar electrodes drives a steady 'a.c. electro-osmotic' fluid flow consisting of two symmetric counter-rotating rolls. Here, and more generally in ICEK, electrodes are patterned onto a substrate (e.g. glass or quartz) using photolithography, such that a sharp boundary between dielectric and metal exists, which gives rise to rapid discontinuities in zeta potential along a planar surface. On a related theme, a uniform a.c. or d.c. electric field induces a dipolar screening cloud around an ideally polarizable particle (Gamayunov, Murtsovkin & Dukhin 1986; Murtsovkin 1996; Squires & Bazant 2004). The action of the field on the screening cloud then drives a quadrupolar induced-charge electro-osmotic (ICEO) flow. If a portion of particle is coated by a thin dielectric layer, the symmetry of the ICEO flow is broken, which causes the particle to translate via induced-charge electrophoresis (ICEP) (Bazant & Squires 2004; Squires & Bazant 2006). Indeed, ICEP of 'metallodielectric' micro-spheres with one dielectric and one metallic hemisphere has been experimentally observed by Gangwal *et al.* (2008). Note, the transition between metal and dielectric portions of the micro-sphere constitutes a sharp variation in zeta potential. Finally, ICEO over a planar electrode was investigated experimentally and theoretically by Soni, Squires & Meinhart (2007); again, here the zeta potential is discontinuous at the ends of the electrode.

In the present work, we propose and investigate a simple paradigmatic model system for electro-osmosis over an inhomogeneously charged surface. Specifically, we consider a uniform d.c. field applied parallel to a plate possessing a discontinuous jump in surface charge, over which resides a binary symmetric electrolyte. For definiteness, we assert the surface charge upstream of the jump to be zero, whereas downstream, the plate is highly charged, meaning that the zeta potential ζ is of much larger magnitude than the thermal voltage scale $k_B T/e$ (here, k_B is Boltzmann's constant, T is the absolute temperature and e is the fundamental charge). As mentioned above,

discontinuous variations in surface charge occur often in microfluidic channels and ICEK. Therefore, while our model system is somewhat idealized, we do expect that the results presented here will be of relevance to a general class of systems possessing sudden changes in surface charge.

Our work builds on the study of Yariv (2004), who considered electro-osmosis over a surface charge discontinuity in the Debye–Huckel, or low-surface-charge, limit $e\zeta/k_BT \ll 1$. Here, a single length scale exists in the problem: the Debye length λ_D over which the diffuse cloud of (counter)-ions screens the surface charge of the plate. On length scales much larger than λ_D, the *bulk* electric field outside the diffuse layer is simply equal to the uniform applied field, and the velocity field possesses a similarity solution. The uniform bulk field drives an ionic surface current through the diffuse layer, whereas the uncharged region upstream of the discontinuity establishes zero surface current, apparently violating ion conservation. To conserve current, ions must be brought into the diffuse layer from the bulk electrolyte, in turn drawing field lines in toward the discontinuity. For a low surface charge, the surface current is small, $O(e\zeta/k_BT)^2$, and thus Yariv's analysis is consistent in the Debye–Huckel limit, i.e. to $O(e\zeta/k_BT)$. However, surface conductivity is no longer small for a highly charged plate, and a significant surface current is carried in the diffuse layer.

The central purpose of our paper is to explore the rather dramatic consequences of imposing ion conservation at the surface charge discontinuity. A simple current-counting argument reveals that the downstream distance required to drive enough ions into the diffuse layer to ensure ion conservation can be surprisingly large. Consequently, the bulk field takes an equally long distance to 'heal' from the jump in surface current and return to the (uniform) applied field. Furthermore, the bulk fluid flow is driven by electro-osmotic slip at the diffuse layer/bulk interface. Hence, as the tangential component of the bulk field is reduced at the discontinuity, the flow also requires a comparably long distance to heal. Surface transport of ions plays an analogous role in electrophoresis: at high zeta potentials, surface transport reduces the tangential field around a particle, which in turn diminishes the driving force for electrophoresis. In fact, for sufficiently high zeta potentials, the electrophoretic mobility decreases with increasing zeta (Dukhin & Deryaguin 1974; O'Brien & White 1978; O'Brien 1983; Russel *et al.* 1989).

In §2, we start with an intuitive physical picture illustrating the mechanism by which surface conduction drives large-scale electric-field gradients in our model system. A simple current-counting argument gives the scaling for the electrokinetic 'healing length.' Scaling by this healing length reduces all such problems to a single universal problem, which we pose and solve numerically in §3. We discuss the results, their implications, and further surprises in §4.

2. Basic physical picture

A definition sketch for electro-osmosis over a flat plate with sudden jump in surface charge is shown in figure 1. In this section, we use simple physical arguments to demonstrate how surface conduction drives large-scale gradients in the bulk electric field. We assert the plate to have a negative zeta potential downstream of the jump ($\zeta < 0$), which attracts a diffuse layer of positively charged (counter)-ions that act to screen the surface charge. The distance over which the screening occurs is characterized by the Debye length λ_D. For a binary, symmetric electrolyte $\lambda_D = \sqrt{\varepsilon k_BT/2c_\infty(ze)^2}$, where c_∞ is the ion concentration far from the plate, ε is the dielectric permittivity,
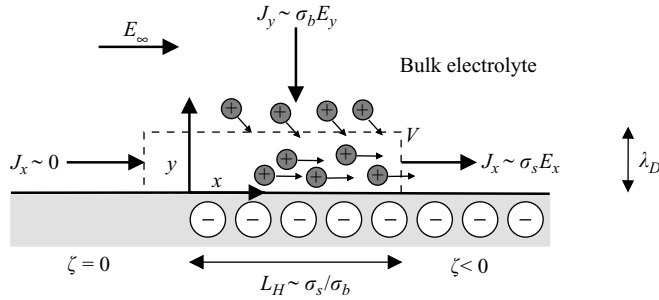
FIGURE 1. Definition sketch for electro-osmosis over a plate with discontinuous variation in surface charge. A uniform field E_∞ is applied tangential to the plate, which we assume has a uniform negative charge downstream of the jump, $\zeta < 0$. A surface current $J_x \sim \sigma_s E_x$ leaves the right-hand side of the control volume V, whereas there is zero current entering from the left-hand side (from the uncharged upstream region). Thus, to conserve ions, a current $J_y \sim \sigma_b E_y$ is delivered into the diffuse layer over an electrokinetic healing length scale L_H, which is equal to the ratio of surface-to-bulk conductivities σ_s/σ_b. After a distance $O(L_H)$ downstream the bulk electric field is once again tangential to the plate.

and z is the valence. For example, a 1 mM monovalent (e.g. KCl) aqueous electrolyte at 298 K gives $\lambda_D \approx 10$ nm.

Consider a uniform electric field applied parallel to the plate, $\boldsymbol{E}_\infty = E_\infty \hat{\boldsymbol{x}}$. The field causes ions to move through electromigration and electro-convection with the local fluid flow, establishing an electrical current in the diffuse layer. Let us examine the conservation of current in a control volume V, which extends vertically from the plate to the diffuse layer/bulk interface and horizontally from the discontiniuity to the healing length L_H (see figure 1). A (depth-integrated) surface current $J_x \sim \sigma_s E_x$ leaves the right-hand side of V, where E_x is the tangential component of the bulk field and σ_s is the surface conductivity (see e.g. Lyklema 1995). However, there is zero surface current entering from the left-hand side. Thus, to ensure ions are conserved, a total current $J_y L_H \sim \sigma_b E_y L_H$ must be supplied into V from the bulk electrolyte, where E_y is the normal component of the bulk field and σ_b is the bulk conductivity. How long must L_H be to draw enough ions into V to match the flux out of the right-hand side? Given that the normal E_y and tangential fields E_x are of the order of the applied field E_∞, equating the surface J_x and normal $J_y L_H$ fluxes gives a healing length $L_H = \sigma_s/\sigma_b$ that is equal to the ratio of surface-to-bulk conductivities. Physically, up to a downstream distance of $O(L_H)$ there is a normal field E_y driving ions into the diffuse layer, after which the field 'heals' and is once again equal to the applied field ($E_y = 0$, $E_x = E_\infty$). Put differently, it takes a distance $O(L_H)$ for the bulk field to 'forget' about the step-change in conductivity.

Formally, conservation of current in a differential volume element within V yields

$$E_y = \frac{\partial}{\partial x} \left(\frac{\sigma_s(x)}{\sigma_b} E_x \right). \tag{2.1}$$

We emphasize that the surface conductivity is spatially dependent; in the present case, $\sigma_s(x)$ is zero upstream of the discontinuity and a finite positive value downstream. It is precisely the jump in surface conductivity that requires ions to be supplied to the diffuse layer, which in turn necessitates a bulk field pointing into the diffuse layer. Thus, non-uniform surface conduction drives gradients in the bulk field. Note, our arguments for the electrokinetic healing length $L_H = \sigma_s/\sigma_b$ are independent of the

specific model for the surface conductivity. As a particular example, for the classic Guoy–Chapman (GC) model of the diffuse layer, the healing length is given by (Bikerman 1940; Lyklema 1995; Chu & Bazant 2007)

$$L_H \equiv \frac{\sigma_s}{\sigma_b} = 4\lambda_D(1+m)\sinh^2\left(\frac{ze\zeta}{4k_BT}\right). \tag{2.2}$$

In the above, ζ is the zeta potential, and m represents the relative contribution of electro-convection to electro-migration in surface conduction; typically, $m \approx 0.1$ (Lyklema 1995). At large zeta potentials, we find $L_H/\lambda_D \sim e^{ze|\zeta|/2k_BT} \gg 1$, i.e. the healing length is much greater than the Debye screening length. For instance, taking $\zeta = 250\,\text{mV}$ and $\lambda = 10\,\text{nm}$ (as is not uncommon in induced-charge electro-osmotic experiments, e.g. of Levitan *et al.* 2005) gives $L_H \approx 1.5\,\mu\text{m}$; thus, even though surface conduction occurs in a nanometre-scale diffuse layer, the effects on the bulk field are considerably more long-range. On the other hand, in the low-zeta-potential limit $L_H/\lambda_D \sim (ze\zeta/2k_BT)^2 \ll 1$; here, L_H is so small that the bulk field heals almost instantaneously and is essentially equal to the uniform applied field Yariv (2004). Before continuing, we note that in the context of electrophoresis the ratio of healing length-to-colloid radius, L_H/a, is known as the Dukhin number Du (Deryagiun & Dukhin 1969; Dukhin 1993; Lyklema 1995). At high Du, the healing length is as big as or greater than the particle radius, and bulk field lines are perpendicular to the (local) diffuse layer/bulk interface.

3. Bulk field and flow

In this section, we compute numerically the bulk electric field, accounting for the non-uniform surface conduction in the diffuse layer by employing (2.1) as an effective boundary condition at the diffuse layer/bulk interface. Assuming that the ion concentration in the electroneutral bulk does not vary, the bulk potential ϕ satisfies Laplace's equation. Far from the charged plate, the potential approaches the imposed field, $\phi \to -E_\infty x$. To non-dimensionalize the problem, we scale distances by the healing length, $L_H = \sigma_s/\sigma_b$, and the potential by $E_\infty L_H$. Thus, the dimensionless governing equation and boundary conditions read

$$\nabla^2\phi = 0, \tag{3.1}$$

$$\phi \to -x \quad \text{as} \quad r = \sqrt{x^2+y^2} \to \infty, \tag{3.2}$$

$$\frac{\partial\phi}{\partial y} = \frac{\partial}{\partial x}\left(h(x)\frac{\partial\phi}{\partial x}\right) \quad \text{at} \quad y = 0, \tag{3.3}$$

where $h(x) = \sigma_s(x)/|\sigma_s|$ is the scaled surface conductivity, and all other variables are also dimensionless. It is worth noting that (3.1)–(3.3) represent a universal system for the bulk field – the only assumption made is that the healing length L_H is much larger than the screening length λ_D, enabling us to replace the detailed diffuse-layer structure with the effective boundary condition (3.3). Of course, the magnitude of L_H depends on the diffuse-layer structure; as shown above, for large zeta potentials, the GC model indeed gives $L_H/\lambda_D \gg 1$. Strictly speaking, the dimensionless surface conductivity $h(x)$ is a Heaviside function, arising from the discontinuity in zeta potential. However, to avoid numerical issues associated with discontinuous boundary conditions, we take $h(x) = [1 + \tanh(\alpha x)]/2$, which approaches the Heaviside function in the limit $\alpha \to \infty$.
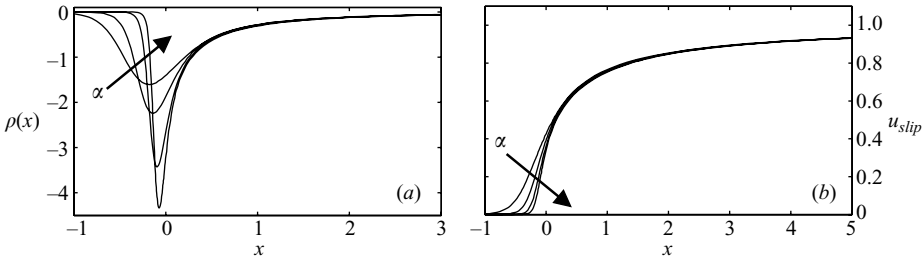
FIGURE 2. (a) Singularity distribution $\rho(x)$, and (b) Dimensionless slip velocity $u_{slip} = -f(x)E_x$. The arrows correspond to increasing α, and solid lines are for $\alpha = 3, 5, 10$ and 15, respectively.

To proceed, we write the potential in terms of the Green's function representation

$$\phi(x_0, y_0) = -x_0 - \frac{1}{4\pi} \int_{-\infty}^{\infty} \rho(x) \ln \left[(x_0 - x)^2 + y_0^2 \right] dx, \qquad (3.4)$$

where $\rho(x)$ is the (as yet unknown) singularity distribution at the diffuse layer/bulk interface. Note, the lower limit of the integral is taken as $-\infty$ as a result of our approximation of the Heaviside function $h(x)$. Substituting (3.4) into the boundary condition (3.3), we find that $\rho(x)$ satisfies

$$\rho(x_0) - \frac{1}{\pi} \int_{-\infty}^{\infty} \rho(x) \left(\frac{h(x_0)}{(x_0 - x)^2} - \frac{1}{x_0 - x} \frac{dh(x_0)}{dx_0} \right) dx = 2 \frac{dh(x_0)}{dx_0}, \qquad (3.5)$$

which is a Fredholm integral equation of the second kind. To solve for $\rho(x)$, we restrict the integral in (3.5) to a finite interval $x \in [-R, R]$ (paying careful attention that the choice of R does not affect the computed value of $\rho(x)$), and then discretize the truncated integral via a Gauss–Legendre quadrature. The resulting linear system of equations for $\rho(x)$ is solved using the Nydstrom method, as outlined in Press *et al.* (1992). Figure 2(a) plots $\rho(x)$ for several values of α.

To compute the bulk field lines, we note that the potential ϕ satisfies the Cauchy–Riemann relations $\partial \phi / \partial x = \partial A / \partial y$ and $\partial \phi / \partial y = -\partial A / \partial x$, where contours of constant A correspond to field lines. Using (3.4), a straightforward calculation gives

$$A(x_0, y_0) = -y_0 - \frac{1}{2\pi} \int_{-\infty}^{\infty} \rho(x) \arctan \left(\frac{y_0}{x_0 - x} \right) dx. \qquad (3.6)$$

In figure 3, we plot the bulk field lines. As we argued physically, ion conservation clearly causes field lines to be directed into the diffuse layer at the location of the jump in surface charge. After an $O(1)$ downstream distance ($O(L_H)$ in dimensional terms), the field heals and is once again parallel to the plate.

Fluid flow in the electroneutral bulk is driven by the electro-osmotic slip at the diffuse layer/bulk interface; the slip velocity is given by the Helmholtz–Smoluchowski formula $u_{slip} = -\varepsilon \zeta E_x / \eta$ (in dimensional variables). For the low Reynolds numbers relevant here, the bulk flow is governed by the homogeneous Stokes equations, which take the dimensionless form

$$\nabla^2 \boldsymbol{u} = \nabla p, \quad \nabla \cdot \boldsymbol{u} = 0, \qquad (3.7)$$

where the velocity $\boldsymbol{u}$ and pressure p are scaled with $\varepsilon \zeta E_\infty / \eta$ and $\varepsilon \zeta E_\infty / L_H$, respectively. The velocity field may be expressed in terms of the
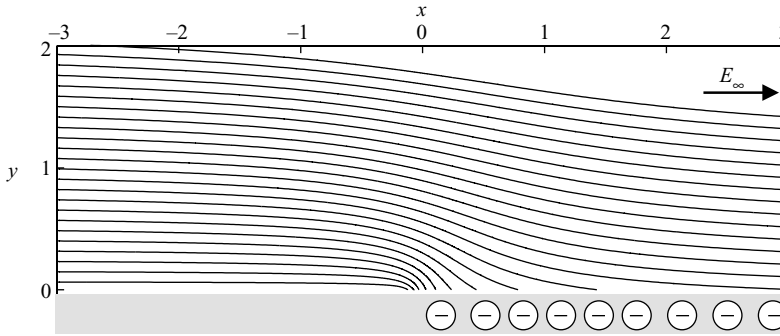
FIGURE 3. Bulk electric field lines over a plate with discontinuous surface charge. Lengths x and y are made dimensionless with the healing length $L_H = \sigma_s/\sigma_b$ and $\alpha = 15$. Notice that the tangential field is greatly reduced at the surface charge discontinuity, as ions must be brought into the diffuse layer from the bulk electrolyte. After a distance $x \sim O(1)$, the field heals and is once again equal to the uniform applied field E_∞.

streamfunction ψ as

$$\boldsymbol{u} = -\frac{\partial \psi}{\partial y}\hat{\boldsymbol{x}} + \frac{\partial \psi}{\partial x}\hat{\boldsymbol{y}}. \tag{3.8}$$

Taking the curl of the Stokes equations, it is found that the streamfunction obeys the biharmonic equation $\nabla^4 \psi = 0$. Additionally, the streamfunction satisfies the slip boundary condition

$$\psi = 0, \quad \frac{\partial \psi}{\partial y} = f(x)E_x \quad \text{at} \quad y = 0, \tag{3.9}$$

where $f(x) = \zeta(x)/|\zeta|$ is the dimensionless zeta potential, which is strictly equal to zero upstream of the discontinuity and minus one downstream. However, to be consistent with our previous computations, we approximate $f(x)$ in the same manner as $h(x)$. In figure 2(b), we plot the slip velocity $-f(x)E_x$, from which it can be seen that our numerical approximation of the step discontinuity produces convergent results for large α. An analytical solution for the streamfunction can be obtained using Fourier transforms; the final result is expressed as a convolution integral

$$\psi(x_0, y_0) = \frac{1}{\pi} \int_{-\infty}^{\infty} f(x)E_x(x)\frac{y_0^2}{y_0^2 + (x_0 - x)^2} \, dx. \tag{3.10}$$

An asymptotic analysis of (3.10) reveals that close to the diffuse layer/bulk interface, $y_0 \to 0$, the streamfunction behaves as $\psi(x_0, y_0) \sim f(x_0)E_x(x_0)y_0$, which satisfies (3.9). Note that in the absence of surface conduction ($|\zeta| \ll 1$), where the tangential field E_x is equal to unity (or the imposed field E_∞, in dimensional terms), (3.10) can be integrated directly to give

$$\psi(x_0, y_0) = -\frac{y_0}{2}\left[1 + \frac{2}{\pi}\arctan\left(\frac{x_0}{y_0}\right)\right], \tag{3.11}$$

which is precisely the similarity solution found by Yariv (2004). This is not surprising, of course, since at low zeta potentials on distances much greater than λ_D there is no length scale in the problem – i.e. for $|\zeta| \ll 1$, the healing length $L_H \ll \lambda_D$.

In figure 4, we plot fluid streamlines over the highly charged plate. It is seen that fluid from upstream is drawn toward the discontinuity in surface charge; streamlines are contracted near the jump, indicating that the flow is accelerating in that region.
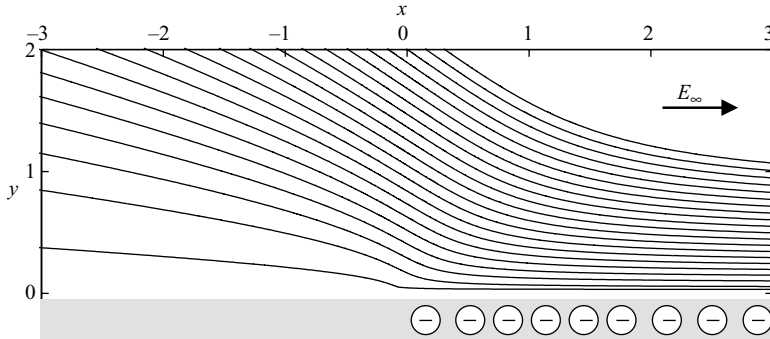
FIGURE 4. Fluid streamlines over a plate with discontinuous surface charge. As in figure 3, $\alpha = 15$. The plate corresponds to $\psi = 0$ and the streamlines are in increments of 0.04.

Downstream of the discontinuity, after a distance $x \sim O(1)$, the electric field heals from the charge discontinuity, as a result, we recover a uniform (plug) flow parallel to the plate.

4. Discussion

Over the last twenty years or so, considerable attention has been paid toward electrokinetic transport over inhomogeneously charged surfaces. In the present work, we investigated a paradigmatic model system for such situations: namely, electro-osmosis over a plate posessing a discontinuity in surface charge. At large zeta potentials, surface transport of ions in the $O(\lambda_D)$-thin screening cloud downstream of the jump profoundly affects the electric field in the bulk electrolyte. Specifically, in order for current to be conserved, ions must be driven into the diffuse layer over a healing length L_H, which is equal to ratio of surface-to-bulk conductivities: $L_H = \sigma_s/\sigma_b$. This in turn requires bulk field lines to be drawn into the diffuse layer at the location of the discontinuity; i.e. surface transport drives gradients in the bulk field. After a distance downstream of $O(L_H)$, the bulk field is once again parallel to the plate. Scaling all distance with the healing length yields a 'universal' problem for the bulk field and fluid flow, which we solved numerically. Note, the region upstream of the jump will more generally possess a non-zero surface charge. In that case, the healing length is $L_H = \Delta\sigma_s/\sigma_b$, where $\Delta\sigma_s$ is the difference between downstream σ_s^D and upstream σ_s^U surface conductivities.

Although our general arguments hold for *any* model of the surface conductivity σ_s, the magnitude of the healing length L_H depends on the specific model for surface conduction in the diffuse layer. For the classic GC model of the diffuse layer, for example, $L_H \sim \lambda_D \sinh^2(ze\zeta/4k_BT)$. At large zeta potentials $L_H \sim \lambda_D e^{ze|\zeta|/2k_BT}$, and thus for reasonable values of the screening length and zeta potential, the healing length may be of the order of micrometres. Hence, this raises the possibility of observing such healing lengths and associated large-scale field gradients in microfluidic experiments. It is important to note, however, that at the heart of the GC model are the assumptions that ions are point-sized and non-interacting. Clearly, this is a significant idealization, which leads to the unrealistic conclusion that the surface conductivity σ_s diverges exponentially at high zeta potentials (physically, since the ions are point-sized, one may 'pack' an infinite number of them into the diffuse layer). Kilic, Bazant & Ajdari (2007) generalized the GC model to account for finite-sized ions, and showed that
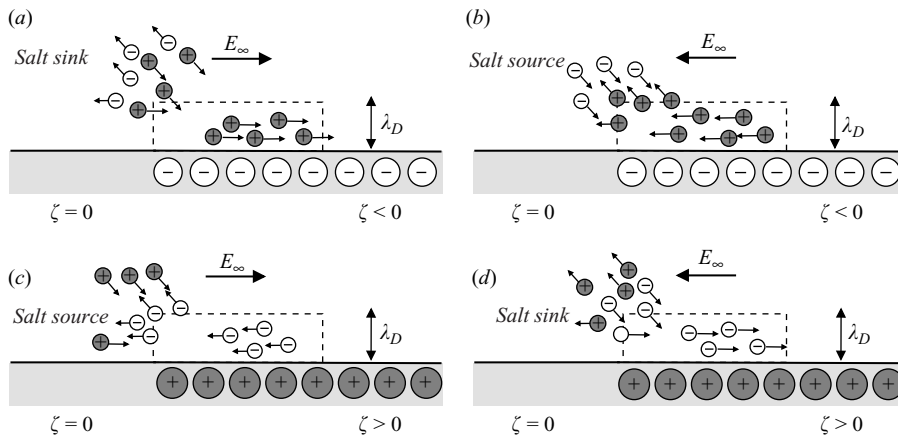
FIGURE 5. Concentration polarization in electro-osmosis over a plate with a sudden jump in surface charge. In (*a*) and (*d*) negative and positive co-ions are driven away from the discontinuity location, respectively, resulting in a salt sink. Conversely, for (*b*) and (*c*), negative and positive co-ions move toward the discontinuity, respectively, yielding a salt source.

surface conductivity increases sub-linearly at high zeta potentials – which would give a smaller healing length than GC. However, we again emphasize the generality of our analysis: once distances are made dimensionless with L_H, the bulk field and flow obey a universal set of equations, which are *independent* of the detailed structure of the diffuse layer.

In this study, we asserted that the downstream region is negatively charged ($\zeta < 0$) and the field is in the positive *x*-direction ($E_\infty > 0$). Hence, at the jump in surface charge, positive counter-ions are driven into the diffuse layer from the bulk (figure 5*a*). What happens if the field is reversed ($E_\infty < 0$)? In this case, in the vicinity of the discontiniuty, positive ions are driven *into* the bulk, along field lines that are drawn *out of* the diffuse layer (figure 5*b*). What happens to this large excess of positive ions? In fact, the bulk field lines drive negative (co)-ions toward the discontinuity, where they join the excess positive ions to increase the local (neutral) salt concentration – a salt source. In our original picture, by contrast, the (negative) co-ions driven along field lines away from the jump in surface charge are not replenished owing to their relative absence within the diffuse layer, yielding a decrease in salt concentration there – a salt sink. Analogously, a downstream region with positive ζ under a field $E_\infty > 0$ has negative counter-ions ejected into the bulk, where positive co-ions join them to form a salt source (figure 5*c*). Lastly, if the field is reversed and ζ is positive, negative ions are drawn into the diffuse layer at the discontinuity and positive ions driven away – a salt sink (figure 5*d*). Importantly, in each case, the sinks and sources are established over the healing length L_H.

Large-scale salt gradients occur routinely in electrokinetic transport over non-uniform surfaces, and are known generically as concentration polarization (see Khair & Squires 2008 and references therein). At steady state, the bulk salt concentration c obeys an advection–diffusion equation

$$D\nabla^2 c = \boldsymbol{u} \cdot \nabla c, \tag{4.1}$$

where D is the ion diffusivity. The relative importance of advection and diffusion is characterized by a Péclet number, $Pe = |\boldsymbol{u}|L_H/D$. For $Pe \equiv 0$, the salt distribution is governed by diffusion only. In this limit, the discontinuity in surface charge presents

a line sink (cases (*a*) and (*d*)) or source (cases (*b*) and (*c*)) of salt. This problem is, in fact, ill-posed: the line sink or source is so strong that the concentration polarization zone extends infinitely far into the bulk, diverging logarithmically. At non-zero *Pe*, however, the bulk flow advects the salt sink or source away from the discontinuity, thereby providing a regularization mechanism that enables a steady-state distribution to be achieved. A purely diffuse steady state is possible, nevertheless, with a plate containing a charged strip of finite width, where the trailing and leading discontinuities in surface charge represent a source–sink line dipole with zero net consumption (or generation) of salt.

However, this is not the whole story: in addition to electro-osmotic slip, salt gradients drive a 'chemi-osmotic' slip flow. As shown by Prieve *et al.* (1984), the slip velocity at the outer edge of the diffuse layer is

$$u_{slip} = -\frac{\varepsilon\zeta}{\eta}\frac{\partial\phi}{\partial x} - \frac{4\varepsilon}{\eta}\left(\frac{kT}{ze}\right)^2 \ln\cosh\left(\frac{ze\zeta}{k_B T}\right)\frac{\partial}{\partial x}\ln\left(\frac{c}{c_\infty}\right), \qquad (4.2)$$

where the first term is the usual electro-osmotic slip, and the second is a chemi-osmotic slip owing to logarithmic gradients in salt concentration. Therefore, the bulk fluid flow is coupled in a nonlinear manner to the salt concentration via (4.1) and (4.2). Furthermore, note that unlike the electro-osmotic slip, whose direction is determined by the sign of $\zeta\partial\phi/\partial x$, chemi-osmotic flow is always to regions of lower salt concentration. For large zeta potentials, chemi-osmosis is of the same 'order' in ζ as electro-osmosis, and thus may significantly contribute to the bulk flow structure. Clearly, the incorporation of concentration polarization effects into our simple universal model system will lead to new, interesting physics. We must, however, leave this for future investigations.

REFERENCES

AJDARI, A. 1995 Electro-osmosis on inhomogeneously charge surfaces. *Phys. Rev. Lett.* **75**, 755.

ANDERSON, J. L. 1985 Effect of non-uniform zeta potential on particle movement in electric fields. *J. Colloid Interface Sci.* **105**, 45.

ANDERSON, J. L. & IDOL, W. K. 1985 Electroosmosis through pores with nonuniformly charged walls. *Chem. Engng Commun.* **38**, 93.

BAZANT, M. Z. & SQUIRES, T. M. 2004 Induced-charge electrokinetic phenomena: theory and microfluidic applications. *Phys. Rev. Lett.* **92**, 066010.

BIKERMAN, J. J. 1940 Electrokinetic equations and surface conductance, a survery of the diffuse double layer theory of colloidal solutions. *Trans. Faraday Soc.* **36**, 154.

CHU, K. T. & BAZANT, M. Z. 2007 Nonlinear electrochemical relaxation around conductors. *Phys. Rev. E* **74**, 011501.

DERYAGUIN, B. V. & DUKHIN, S. S. 1969 Theory of surface conductance. *Colloid J. USSR* **31**, 277.

DUKHIN, S. S. 1993 Non-equilibrium electric surface phenomena. *Adv. Colloid Interface Sci.* **44**, 1.

DUKHIN, S. S. & DERYAGUIN, B. V. 1974 Electrokinetic phenomena. *Surface and Colloid Science* 7 (ed. E. Matijevic). Wiley.

GAMAYUNOV, N. I., MURTSOVKIN, V. A. & DUKHIN, A. S. 1986 Pair interaction of particles in electric field. 1. Features of hydrodynamic interaction of polarized particles. *Colloid J. USSR* **48**, 197.

GANGWAL, S., CAYRE, O. J., BAZANT, M. Z. & VELEV, O. D. 2008 Induced-charge electrophoresis of metallodielectric particles. *Phys. Rev. Lett.* **100**, 058302.

GHOSAL, S. 2006 Electrokinetic flow and dispersion in capillary electrophoresis. *Annu. Rev. Fluid Mech.* **38**, 309.

GONZÁLEZ, A., RAMOS, A., GREEN, N. G., CASTELLANOS, A. & MORGAN, H. 2000 Fluid flow induced by nonuniform ac electric fields in electrolytes on microelectrodes. II. A linear double-layer analysis. *Phys. Rev.* E **61**, 4019.

VAN DER HEYDEN, F. H. J., BONTHUIS, D. J., STEIN, D., MEYER, C. & DEKKER, C. 2006 Electrokinetic energy conversion efficiency in nanofluidic channels. *Nano. Lett.* **6**, 2232.

VAN DER HEYDEN, F. H. J., BONTHUIS, D. J., STEIN, D., MEYER, C. & DEKKER, C. 2007 Power generation by pressure-driven transport of ions in nanofluidic channels. *Nano. Lett.* **7**, 1022.

KHAIR, A. S. & SQUIRES, T. M. 2008 Fundamental aspects of concentration polarization arising from non-uniform electrokinetic transport. *Phys. Fluids* **20**, 087102.

KHANDURINA, J. & GUTTMAN, A. 2003 Microscale separation and analysis. *Curr. Opin. Chem. Biol.* **7**, 595.

KILIC, M. S., BAZANT, M. Z. & AJDARI, A. 2007 Steric effects in the dynamics of electrolytes at large applied voltages. I. Double-layer charging. *Phys. Rev.* E **75**, 021502.

KIM, S. J., WANG, Y. C., LEE, J. H., JANG, H. & HAN, J. 2007 Concentration polarization and nonlinear electrokinetic flow near a nanofluidic channel. *Phys. Rev. Lett.* **99**, 044501.

LEVITAN, J. A., DEVASENATHIPATHY, S., STUDER, V., BEN, Y., THORSEN, T., SQUIRES, T. M. & BAZANT, M. Z. 2005 Experimental observation of induced-charge electro-osmosis around a metal wire in a microchannel. *Colloids Surfaces* A **267**, 122.

LONG, D. & AJDARI, A. 1998 Symmetry properties of the electrophoretic motion of patterned colloidal particles. *Phys. Rev. Lett.* **81**, 1529.

LONG, D., STONE, H. A. & AJDARI, A. 1999 Electroosmotic flows created by surface defects in capillary electrophoresis. *J. Colloid Interface Sci.* **212**, 338.

LYKLEMA, J. 1995 *Fundamentals of Interface and Colloid Science. Volume II: Solid–Liquid Interfaces.* Academic.

MURTSOVKIN, V. A. 1996 Nonlinear flows near polarized disperse particles. *Colloid J. Russ. Acad. Sci.* **53**, 947.

O'BRIEN, R. W. 1983 The solution of the electrokinetic equations for colloidal particles with thin double layers. *J. Colloid Interface Sci.* **92**, 204.

O'BRIEN, R. W. & WHITE, L. R. 1978 Electrophoretic mobility of a spherical colloidal particle. *J. Chem. Soc. Faraday Trans.* II **74**, 1607.

PENNATHUR, S., EIJKEL, J. C. T. & VAN DER BERG, A. 2007 Energy conversion in microsystems: is there a role for micro/nanofluidics? *Lab. Chip* **7**, 1234.

PRESS, W. H., TEUKOLSKY, S. A., VETTERLING, W. T. & FLANNERY, B. P. 1992 *Numerical Recipes in FORTRAN*, 2nd edn. Cambridge University Press.

PRIEVE, D. C, ANDERSON, J. L., EBEL, J. P. & LOWELL, M. E. 1984 Motion of a particle generated by chemical gradients. Part 2. Electrolytes. *J. Fluid Mech.* **148**, 247.

RAMOS, A., MORGAN, H., GREEN, N. G. & CASTELLANOS, A. 1998 AC electrokinetics: a review of forces in microelectrode structures. *J. Phys.* D **31**, 2338.

REUSS, F. 1809 Sur un nouvel effet de le électricité glavanique. *Mém. Soc. Imp. Nat. Mosc.* **2**, 327.

RICE, C. & WHITEHEAD, R. 1965 Electrokinetic flow in a narrow cylindrical capillary. *J. Phys. Chem.* **69**, 4017.

RUSSEL, W. B., SAVILLE, D. A. & SCHOWALTER, W. R. 1989 *Colloidal Dispersions.* Cambridge University Press.

SONI, G., SQUIRES, T. M. & MEINHART, C. D. 2007 Nonlinear effects in induced charge electroosmosis. *Proc. IMECE2007*, Paper IMECE2007-41468, 2007 ASME International Mechanical Engineering Congress and Exposition, Seattle, WA, USA.

SQUIRES, T. M. & BAZANT, M. Z. 2004 Induced-charge electro-osmosis. *J. Fluid Mech.* **509**, 217.

SQUIRES, T. M. & BAZANT, M. Z. 2006 Breaking symmetries in induced-charge electro-osmosis and electrophoresis. *J. Fluid Mech.* **560**, 65.

SQUIRES, T. M. & QUAKE, S. 2005 Microfluidics: fluid physics at the nanoliter scale. *Rev. Mod. Phys.* **77**, 977.

STONE, H. A., STROOCK, A. D. & AJDARI, A. 2004 Engineering flows in small devices: microfluidics toward a lab-on-a-chip. *Annu. Rev. Fluid Mech.* **36**, 381.

STOREY, B. D., EDWARDS, L. R., SABRI KILIC, M. & BAZANT, M. Z. 2008 Steric effects on ac electro-osmosis in dilute electrolytes. *Phys. Rev.* E **77**, 036317.

STROOCK, A. D., WECK, M., CHIU, D. T., HUCK, W. T. S., KENIS, P. J. A., ISMAGILOV, R. F. & WHITESIDES, G. M. 2000 Patterning electro-osmotic flow with patterned surface charge. *Phys. Rev. Lett.* **84**(15), 3314.

TEUBNER, M. 1982 The motion of charge colloidal particles in electric fields. *J. Chem. Phys.* **76**, 5564.

WANG, Y., STEVENS, A. & HAN, J. 2005 Million-fold preconcentration of proteins and peptides by nanofluidic filter. *Anal. Chem.* **77**, 4293.

YARIV, E. 2004 Electro-osmotic flow near a surface charge discontinuity. *J. Fluid Mech.* **521**, 181.